5677

Focused Source EM Survey – New Solution for Both Shallow and Deep Water

S. Davydycheva* (R&D 3D EM Consulting) & N.I. Rykhlinski (Institute of Innovative Methods of Geophysics)

SUMMARY

A new Focused Source Electromagnetic (FSEM) method exploits an idea of focusing the EM field in vertical direction and thus can provide the deep-reading resistivity data. It allows directing the EM energy into the formation, similar to the acoustic beam used in the seismic exploration. Thus, it enables higher spatial resolution and greater depth of investigation than the conventional CSEM method. In addition to the formation resistivity, FSEM can provide spectral properties of the resistivity affected by the Induced Polarization effect. Both modeling and field examples demonstrate high efficiency of FSEM.

Introduction

In spite of the progress in seismic prospecting methods for oil and gas exploration on the continental shelf, these methods may be not sufficient to reliably detect and delineate hydrocarbon reservoirs, especially of medium and small sizes. Therefore, it is important to get any additional geophysical information that could reduce financial risks associated with expensive drilling on the shelf.

A new Focused Source Electromagnetic (FSEM) survey exploits an idea of focusing the EM field in vertical direction and thus provides the deep-reading resistivity data. Its theoretical background for axial setup was given by Davydycheva et al. (2006). The focusing has been used in EM well logging (Doll, 1951) to increase the spatial resolution and the depth of investigation. Similar to the acoustic beam used in the seismic exploration, it allows to direct the EM energy into the formation. We apply it on the shelf or on the earth surface.

In addition to the resistivity data, the FSEM can provide spectral properties of the formation resistivity. They may be nontrivial in the presence of the induced polarization (IP) effect, which strongly affects low-frequency or late-time transient responses.

The method started its development as a land or shallow-water marine survey. The airwave effect that can mask the reservoir response in shallow water when applying the standard Controlled Source EM (CSEM) technique (Johansen et al, 2005) is removed in our approach. Thus, marine FSEM is successful at both deep and shallow sea water and enables delineating hydrocarbon reservoirs at high depth of hydrocarbons below the sea floor.

Methodology

The method is based on the complete elimination at the receiver of the both horizontal components of the electric current density j. This feature provides high spatial resolution of the method and its high sensitivity to deep structures. For this purpose, both conventional dipole and multi-electrode quadrupole receivers are used (see Davydycheva et al. 2006).

The geological formation is excited by consequent rectangular pulses of the electromagnetic field with pauses between them. When the current is on, the geometrical sounding is performed in a wide range of the setup offsets (from hundreds meters to kilometers), whereas the transient response of the formation is measured during the off-time. Thus, two sets of data are derived from the measurements. The first one, $R_{xy}(x,t_0)$, comes from the geometrical sounding, when the transmitter current is on. It allows determining the formation resistivity ρ. It may reflect the presence of hydrocarbon-bearing rocks, which are often more resistive than surrounding rocks. The second set of data $R_{xy}(x,t)$ comes from the transient response of the formation and reflects the spectral properties of the formation resistivity: namely, the IP coefficient η and the time decay constant τ. Typically, they are equal to 0 in many resistive rocks, such as basalt, carbonates, or rock-salt, but have an anomaly in hydrocarbon-bearing rocks. At least, taking the IP parameters into account provides obtaining reliable resistivity data, since they affect late-time responses.

Special care is taken to remove noise by means of accumulation of signals coming from consequent pulses. It is performed until the noise is suppressed below 5%.

Examples: FSEM versus standard CSEM

Let us compare modeling results of FSEM versus the conventional CSEM method, sometimes called Sea Bed Logging. For the modeling we use a 3D finite-difference (FD) method by Davydycheva and Druskin (1995) and Davydycheva et al. (2003). Due to the material averaging, it requires FD grid to be neither fine nor conformal to interfaces that allows accurate modeling dipping interfaces (see complex bathymetry test: Zaslavsky et al., 2006).

Fig. 1 shows responses of a 3D model of hydrocarbon reservoirs situated 1 km below the seafloor and 0.2 km below the sea surface. The modeled structures approximate typical shape and sizes of actual oil reservoirs. Their resistivity is 50 Ω·m, and dimensions, in km, follow: larger prism has vertices at $x_1 = -5$, $z_1 = 1.4$; $x_2 = -4$, $z_2 = 1.2$; $x_3 = 0$, $z_3 = 1.2$ and $x_4 = 1$, $z_4 = 1.4$; $-3 < y < 3$; smaller prism: $x_1 = 2$, $z_1 = 1.4$; $x_2 = 3.5$, $z_2 = 1.2$, and $x_3 = 5$, $z_3 = 1.4$; $-1.5 < y$

< 1.5. Receivers are situated on the seafloor, at y = 0 and z = 0.2, whereas the horizontal dipole transmitters – at z = 0.17 km. We vary their x-coordinate, keeping the constant offset.

We show relative, or normalized responses, i. e. our measurement R_{xy} (x,t_0) (FSEM) and the electric field $E_x(x)$ (CSEM), both divided by the responses measured at a reference point situated far enough from the reservoir. This allows vizualizing the anomalies above the reservoirs. It is easy to see that our focusing technique provides a clear response of both big and small structures even in the DC case (red curves), whereas the standard CSEM provides both smaller anomalies and lower spatial resolution (blue curves). It becomes apparent that varying the frequency does not really help in improving the spatial resolution: at all frequencies the response of the smaller structure cannot be distinguished from the response of the larger one. Moreover, the smaller structure's response at the highest frequency of 1 Hz is practically absent due to the dominating airwave, since this is a relatively shallow-water case. At zero frequency (DC), even though the airwave is absent and does not mask the responses of both reservoirs, the separation betweem them is still low. The reason is that the spatial resolution of the standard CSEM is restricted by **min** (offset, wavelength). Here we have the wavelenght in the seafloor of 6.3 km at 0.25 Hz that is longer than the offset of 5.2 km in any case. At 1 Hz the wavelength is 3.2 km, but the responses are dominated by the airwave.

Since the focusing technique provides high sensitivity to a relatively narrow column of the rocks below the receiver, its spatial resolution is not restricted by the offset anymore even in the DC case. (The sensitivity function will be shown during the presentation.)

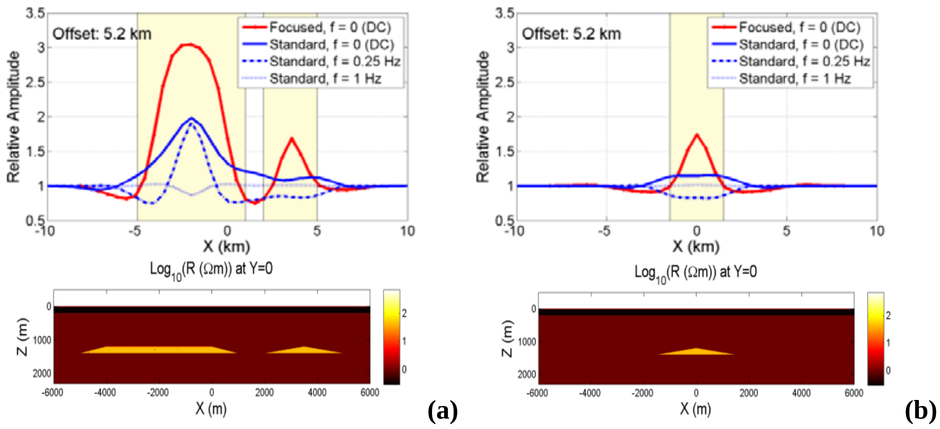

Figure 1: *Water depth 200 m: response of two structures situated 1 km below the seafloor (a), and of the smaller structure only (b). In the bottom: the corresponding 3D models: white: air; black: water, 0.3 Ωm; brown: seafloor, 1 Ωm; orange: 50 Ωm hydrocarbons.*

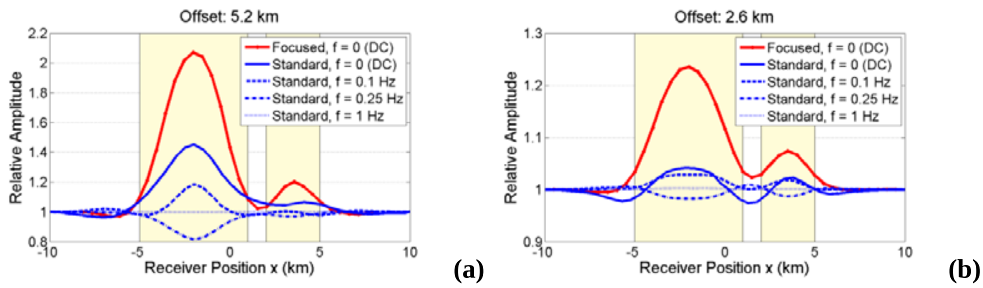

Figure 2: *Water depth 50 m: response of two reservoirs situated 2 km below the seafloor.*

The next modeling example assumes the same structures, as depicted in the bottom of Fig. 1a, but now they are situated deeper: 2 km below the seafloor, with the shallower, only 50 m, water. For the standard CSEM it is a very challenging case due to the strong airwave and the skin-effect. Receivers are on the seafloor, at z = 50 m, and the transmitter is in the water, at z = 20 m. Fig. 2 shows FSEM versus the standard CSEM for the offsets of 5.2 km and 2.6 km. It becomes evident that FSEM with a 5.2 km offset provides very clear reservoir responses:

about 100% above the larger structure and about 20% above the smaller one, and they can be clearly distinguished from each other. The standard CSEM response has an anomaly of 45% above the larger structure, but the smaller one is virtually lost in its "shade". Varying the excitation frequency is completely useless in this case: non-zero frequency does not seem to provide any additional information, and only reduces the CSEM response, as compared to zero-frequency response, due to the airwave and the skin-effect. Shorter offset of 2.6 km (Fig. 2b) provides a better spatial resolution of CSEM; however, the size of the anomaly does not exceed 5% **-** too little to be reliably detected. On the other hand, FSEM anomaly approaches 25% for the short offset.

It is worth mentioning that in two shallow-water cases discussed above a visual interpretation of the standard CSEM is questionable. The shape of the responses varies in a complicated way depending on the frequency and the offset. This makes a time-consuming 3D inversion of multi-frequency data necessary. In contrast, the FSEM method allows a simple visual interpretation based on shape of the responses following simple logic.

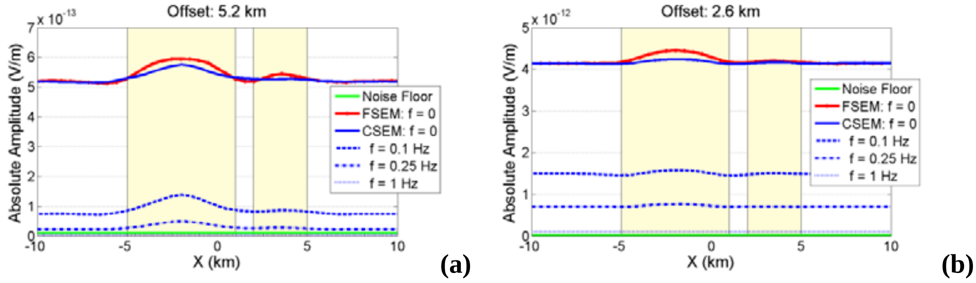

Figure 3: *Deep-water case. Response of two reservoirs situated 2 km below the seafloor.*

Let us examine the applicability of FSEM in deep water. The last modeling example assumes the same structures, as depicted in the bottom of Fig. 1a, situated 2 km below the seafloor, but the water is infinitely deep. Again, the receivers are situated on the seafloor; the transmitter – 30 m above it. Fig. 3 shows relative amplitudes of FSEM versus CSEM. This time we plot absolute amplitudes, since the signal level should be watched in deep water due to strong skin-effect. Fig. 3a shows that for 5.2 km offset the signal at the fundamental CSEM frequency of 0.25 Hz approaches the noise floor, 1.E-14 V/m. Moreover, the signal at the highest frequency, 1 Hz, varies below 1.E-15 V/m – at least one order below the noise floor. Thus, the ability of the standard CSEM technique to provide reliable resistivity data in deep structures such as 2 km below the seafloor is doubtful. However, FSEM still seems promising in this challenging case and so looks successful in deep water as well.

In all the modeling examples we show only the DC responses of FSEM data and prove that even in the DC case it has a great advantage as compared to the standard CSEM. However, additional frequency- or time-domain measurements can provide additional data about the formation. So we also analyze transient responses during the off-time, since they provide the whole spectrum of frequencies. At this stage it is important to take into account the IP effect, since it makes time decay much slower and may strongly affect late-time responses.

Fig. 4 illustrates 1D inversion results of field data obtained at Tympuchikan Gas-condensate Deposit, Eastern Siberia. It presents many 1D images obtained independently and then stitched together, since high spatial resolution of the FSEM enables applying simple 1D inversion for 1D layered medium at each measurement point. It was a land survey, so it would be very challenging for CSEM due to a strong airwave effect. However, application of FSEM enables reliable estimation of the conductivity in the water- and oil-bearing sandstone below more than 1500 m of high-resistive rocks, mostly carbonates, and 200 m of permafrost. High resolution of the method enabled distinguishing oil-bearing sandstone areas of moderate size over 2.5 km in diameter. Two areas of the elevated IP coefficient η – one in the permafrost zone, close to the earth surface, and the other one at the depth of 1750 m – correspond to two geological traps. We believe that η in the upper trap has an anomalous value due to the halo diffusion of hydrocarbons, whereas in the lower one – due to the hydrocarbon reservoir itself.

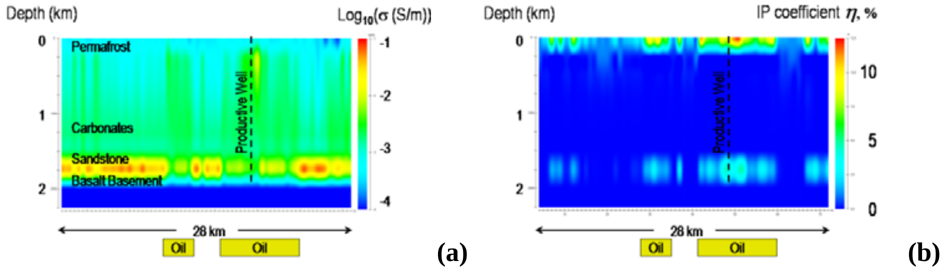

Figure 4: *Tympuchikan Gas-condensate Deposit, Eastern Siberia: 1D inversion results for the electric conductivity (a) and the IP coefficient η (b).*

Conclusions

The new FSEM method has a great potential for revealing and delineating deep hydrocarbon reservoirs of any size on the continental shelf where the standard CSEM method fails to provide reliable results. The cornerstone of the FSEM is its ability to direct the EM energy deep into the geological formation. The new method provides:

- Great depth of investigation and high sensitivity to deep resistive structures;
- Applicability of a simple 1D inversion due to high spatial resolution;
- Removing the masking effects of the airwave and of the high conductive sea water;
- Ability to exploit the IP effect that can provide additional data about the formation;
- High signal-to-noise ratio;
- Possibility of a simple visual interpretation.

Let us recall a history of resistivity well logging. It has come a long way from the first primitive logging devices, giving only an approximate estimate of the formation resistivity in shallow zone around the borehole, to modern focusing tools like Laterolog suggested by Doll (1951). The latter exploits the idea of focusing the electric current that can be re-directed from the highly conductive borehole into the more resistive formation. Application of this method enables a greater depth of investigation and a higher spatial resolution.

We suggest a simple implementation of the similar focusing idea on the seafloor or on the land that not only enables increasing the depth of investigation and the spatial resolution of the method; it also allows removing the airwave effect in shallow water application. Unlike the Laterolog, our focusing technique does not require any automatic feedback loop.

It is worth mentioning that exceptionally large structures such as the Shtockman structure in the Barents Sea, or the Troll West Gas Province (Johansen et al, 2005) typically do not require any additional post-seismic verification for the presence of hydrocarbons.

References

Davydycheva, S. and Druskin, V. [1995] Staggered grid for Maxwell's equations in arbitrary 3-D inhomogeneous anisotropic media. *Proc. Int. Symp. on Three-Dimensional Electromagnetics, Schlumberger-Doll Research, Ridgefield, CT*, 181–187.

Davydycheva, S., Druskin, V., and Habashy, T. [2003] An efficient finite-difference scheme for electromagnetic logging in 3D anisitropic inhomogeneous media, *Geophysics,* **68**, 1525-1536.

Davydycheva, S., Rykhlinski, N., Legeido, P. [2006] Electrical-prospecting method for hydrocarbon search using the induced polarization effect, *Geophysics,* **71,** G179-G189.

Doll, H.G. [1951] The Laterolog: A new resistivity logging method with electrodes using an automatic focusing system. *Petroleum Transactions: AIME*, **192**, 305-316.

Johansen, S.E., Amundsen, H.E.F., Røsten, T., Ellingsrud, S., Eidesmo, T., and Bhuyian, A.H. [2005] Subsurface hydrocarbons detected by electromagnetic sounding. *First Break,* **23**, March, 31-36.

Zaslavsky, M., Davydycheva, S., Druskin, V., Abubakar, A., Habashy, T., and Knizhnerman, L. [2006] Finite-difference solution of 3D EM problem with divergence-free preconditioners. *SEG expanded abstract, 76th annual meeting, New Orleans.*